International Journal of Astronomy and Astrophysics, 2026, 16(3), 145-160
https://www.scirp.org/journal/ijaa
ISSN Online: 2161-4725
ISSN Print: 2161-4717

Study of Warm Dark Matter with the Lyman-α Forest

Bruce Hoeneisen

Universidad San Francisco de Quito, Quito, Ecuador
Email: bhoeneisen@usfq.edu.ec

How to cite this paper: Hoeneisen, B. (2026) Study of Warm Dark Matter with the Lyman-α Forest. *International Journal of Astronomy and Astrophysics*, **16**, 145-160.
https://doi.org/10.4236/ijaa.2026.163010

Received: May 2, 2026
Accepted: July 17, 2026
Published: July 20, 2026

Abstract

Quasar light becomes absorbed by the Lyman-α line of neutral hydrogen in "clouds" along the line-of-sight in the highly ionized intergalactic medium after re-ionization. The received flux spectrum is known as the "Lyman-α forest". Limits on the dark matter "standard thermal relic mass" have been obtained in the literature from the power spectrum of the Lyman-α forest, *e.g.* $m_{\text{th}} > 5.7$ keV. These limits are in tension with four independent estimates of the dark matter warmness: $0.6 \lesssim m_{\text{th}} \lesssim 1.6$ keV. To try to understand this tension we attempt to measure the dark matter warmness by two methods: the power spectrum of the Lyman-α forest, and the width of individual absorption lines, *e.g.* "Lyman-α trees". We obtain a measurement of the dark matter warmness with the Lyman-α forest power spectrum, in agreement with the four independent estimates. In conclusion, the warm dark matter free-streaming is clearly observed as a cut-off of the Lyman-α forest power spectrum.

Keywords

Lyman-α Forest, Warm Dark Matter, Free Streaming, Dark Matter

1. Introduction

About 5/6 of the matter of the universe is in a "dark matter" form that appears to only have the gravitational interaction. If dark matter is composed of particles, the mass of these particles is unknown in the range 10^{-22} eV to 10^{67} eV, *i.e.* over 89 orders of magnitude [1]! The ΛCDM cosmology model assumes dark matter is cold. Never-the-less, we would like to know just how cold or warm dark matter is in order to be able to extrapolate our understanding of the universe to the remote past.

A summary of four largely independent estimates of the dark matter warmness can be found in **Table 3** of [2]. These measurements are consistent with a dark matter "standard thermal relic mass" $0.6\ \text{keV} \lesssim m_{\text{th}} \lesssim 1.6\ \text{keV}$ (defined by Equations (6) and (7) of [3]). This result turns out to be in tension with several published limits on m_{th} summarized in **Figure 3** of [4]. In particular, reference [5] obtains the limit $m_{th} > 5.7$ keV (at 95% confidence) by studying the power spectrum obtained in [6] from dedicated high resolution observations with the Visual Echelle Spectrograph VLT/UVES [7], and the High Resolution Echelle Spectrometer Keck/HIRES [8], in the redshift range $4.2 \lesssim z \lesssim 5.0$.

Let us recall that after re-ionization the universe is highly ionized with a fraction of neutral hydrogen n_{HI}/n_H of order 10^{-4} [9]. This neutral hydrogen absorbs the light of background quasars at the proper (or laboratory) wavelength $\lambda_\alpha = 1215.67$ Å, corresponding to the Lyman-α transition from the ground state $n = 1$ to excited states $n = 2$. Due to the expansion of the universe, the absorption by neutral hydrogen "clouds" along the line-of-sight is observed redshifted on Earth. The resulting flux spectra is known as the "Lyman-α forest".

The purpose of the present study is to try to understand the tension between the measurements summarized in [2], and the limit obtained in [5]. To this end we analyze the Lyman-α power spectrum as in [5]. We also study individual "trees" of the forest, *i.e.* individual absorption lines.

Cross-checking the warm dark matter power spectrum cut-off k_{fs} is difficult due to the non-linear regeneration of the power spectrum, as shown in **Figure 4** of [10]. Never-the-less, the results in **Table 3** of [2] are consistent with cosmic shear measurements (KIDS-Legacy data) [11], and with gravitational lensing of the cosmic microwave backgroud from the Atacama Cosmology Telescope and lensing of galaxies from the Dark Energy Survey [12].

The outline of the article is as follows. Section 2 describes the Lyman-α forest. Section 3 describes the 3D density power spectrum and the 1D Lyman-α forest power spectrum, with their cut-offs due to the warm dark matter free-streaming (and baryon thermal motion). Section 4 estimates each of these contributions. Section 5 presents a measurement of the warmness of the dark matter with the Lyman-α forest power spectrum. Section 6 suggests a measurement method with individual "trees". Conclusions follow. Appendices present parameter definitions and notation, and calculations of the power spectrum cut-off wavevector k_{fs}, the warm dark matter free-streaming length l_{fs}, the masses M_{hm} and M_J, and the relation between 1D and 3D power spectra.

2. The Lyman-α Forest and Sidebands

Neutral hydrogen atoms absorbe (and re-emit isotropically) photons at the proper Lyman-α wavelength 1215.67 Å from background quasars or galaxies, that are "observed" as redshifted missing flux F on Earth. A typical Lyman-α forest is shown in **Figure 1**. Most of the flux power distribution looks like the top panel in **Figure 1**. A few individual absorption lines stand out of the "noise" as shown in the middle and bottom panels of **Figure 1**. In fact, for quasar J140501+444800 we find only 10 absorption lines that appear to be above the "noise" in the wavelength range 5000 Å to 6095 Å. Narrow absorption lines may be part of larger structures as shown in **Figure 2**. We will study in more detail this Lyman-α forest sideband in Section 6.

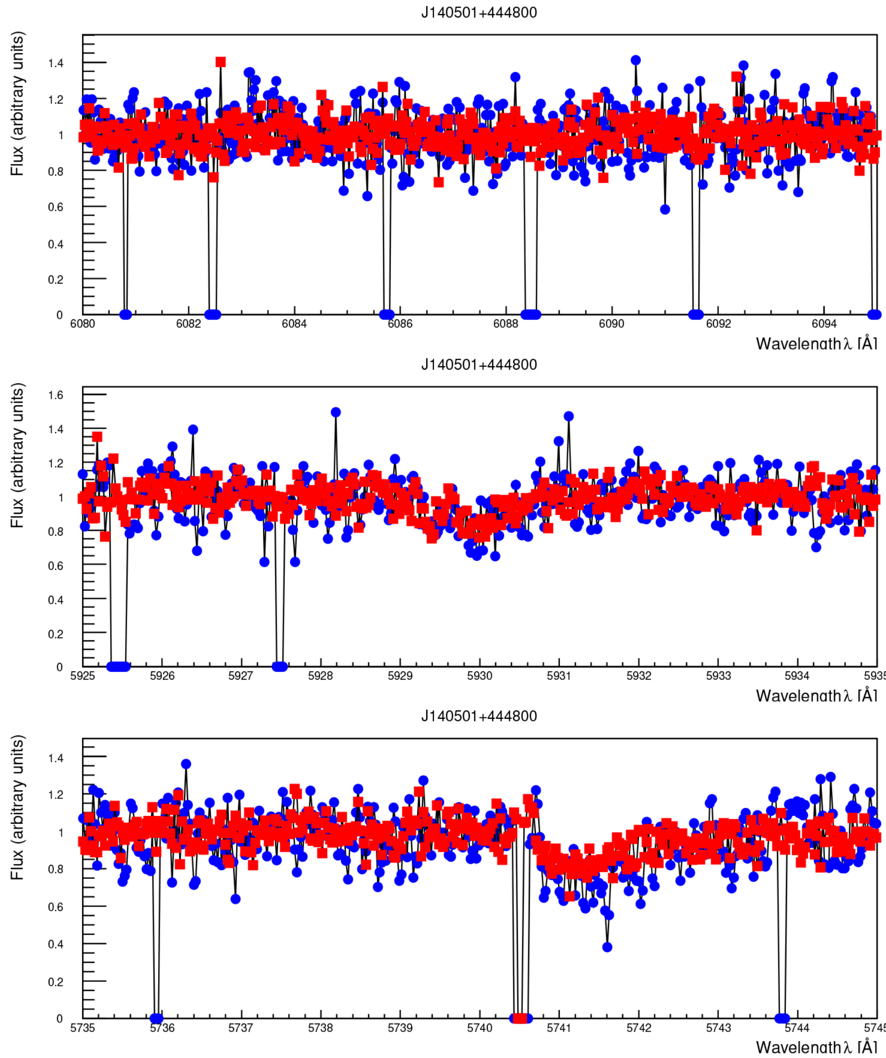

Figure 1. Details of the observed electromagnetic flux from quasar J140501+444800 as a function of wavelength [Å]. Blue (red) corresponds to spectra observed on May 16 (20), 2005, by the Keck Observatory. Data from KODIAQ [13]-[15] at https://koa.ipac.caltech.edu/applications/KODIAQ/kodiaqQSOList.html.

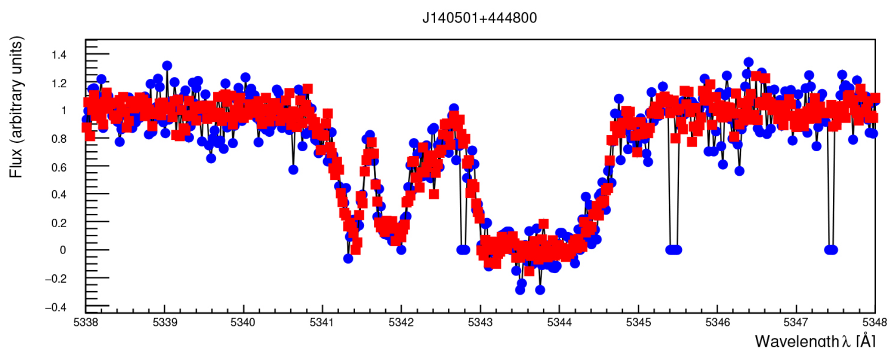

Figure 2. Details of the observed electromagnetic flux from quasar J140501+444800 as a function of wavelength [Å]. Blue (red) corresponds to spectrum observed on May 16 (20), 2005. Data from KODIAQ [13]-[15] at https://koa.ipac.caltech.edu/applications/KODIAQ/kodiaqQSOList.html.

3. Density Power Spectrum $P_{3\text{D}}(k)$ and Lyman-α Forest Power Spectrum $P_{1\text{D}}(k_z)$

Let $P_{\text{CDM}}(k)$ be the power spectrum of density fluctuations in the ΛCDM cold dark matter cosmology. If dark matter is warm, dark matter particles free-stream into, or out of, density minimums and maximums, thereby erasing small scale structure. For warm dark matter the power spectrum becomes

$$P_{3\text{D}}(k) = P_{\text{CDM}}(k)\tau^2(k), \tag{1}$$

where $\tau^2(k)$ is a cut-off factor. See Appendix C for the mathematical details. We will approximate $\tau^2(k)$ to a Gaussian cut-off, so

$$P_{3\text{D}}(k) \equiv P_{\text{CDM}}(k)\exp\left(-\frac{k^2}{k_{\text{fs}}^2}\right). \tag{2}$$

(This is our definition of k_{fs}: $\tau^2(k_{\text{fs}}) \equiv 1/e$. Alternative definitions in the literature are $\tau^2(k_{\text{fs}}) = 1/2$ or 1/4.) We are interested in measuring the wavevector cut-off k_{fs}.

Let $P_\alpha(k_z)$ be the power spectrum of the Lyman-α forest in a cold dark matter and cold baryon scenario. This power spectrum becomes cut-off due to the thermal velocities of both dark matter and baryons. Again we will approximate the cut-off factors to Gaussians. We will use the notation of [9] and [16]. Then the observed comoving

$$P_{1\text{D}}(k_z) \equiv P_\alpha(k_z)\exp\left(-\frac{k_z^2 a^2 b^2}{2}\right). \tag{3}$$

(Later, we will improve on the Gaussian approximation by deriving $P_{1\text{D}}(k_z)$ from $P_{3\text{D}}(k)$ as explained in Appendix F.) b^2 has independent contributions from the Doppler shift due to the thermal velocities of the neutral hydrogen atoms (b_T^2), from pressure (or Jeans) smoothing of baryons (b_ρ^2), from the size of linear expanding neutral hydrogen "clouds" along the line of sight related to dark matter free-streaming (b_{DM}^2), and from the resolution of the spectrograph (b_s^2). The natural width of the Lyman-α transition is negligible. The total variance of independent uncertainties is the sum of variances:

$$b^2 = b_T^2 + b_\rho^2 + b_{\text{DM}}^2 + b_s^2. \tag{4}$$

The intergalactic medium has a position-dependent baryon gas temperature $T = T_0\left(\rho/\langle\rho\rangle\right)^{\gamma-1} \equiv T_0\Delta^{\gamma-1}$. For a noble gas, $\gamma = 5/3$. For the ionized universe, protons and electrons interact with light and approach thermal equilibrium. So, for the highly ionized universe we expect $\gamma \approx 1$ after re-ionization, varying asymptotically to 1.6 at low z. The mean temperature T is measured to be 7000 K to 8000 K [6].

4. Contributions to b^2

The contribution b_T^2 due to the thermal velocities of neutral hydrogen atoms is [9] [16]

$$b_T^2 = \frac{2k_B T}{m_H} = (12.8\ \text{km/s})^2 \left(\frac{T_0}{10^4\ \text{K}}\right) \Delta^{\gamma-1}. \tag{5}$$

The factor 2 is because $b/\sqrt{2}$ is a standard deviation.

The spectrograph nominal resolution is (2.55 km/s [6] [13]) so

$$b_s^2 = \left(\sqrt{2} \cdot 2.55\ \text{km}/s/a\right)^2. \tag{6}$$

Consider a cloud of total (dark matter plus baryon) mass M in the intergalactic medium, that is still linear and expanding. Let $2R$ be a typical proper length of this cloud along the line of sight. For warm dark matter, the minimum mass M that will eventually collapse due to its own gravity is M_{hm}, see Appendix E. If the Jeans mass M_J is less than M, as is our case of interest, the collapse will occur with the full complement of baryons, see Appendix E. After re-ionization, only a fraction of order 10^{-4} of the hydrogen in the cloud will be neutral. If one of these neutral hydrogen atoms absorbes a photon of wavelength λ_α, then, this photon will be "seen" on Earth as a missing photon of redshifted wavelength $\lambda = \lambda_\alpha / a = \lambda_\alpha (1+z)$. Due to the expansion of the cloud, the absorption line will have a width. Let

$$\left(\frac{\hat{\lambda} - \lambda_0}{\lambda_0}\right)_\text{cloud} = \left(\frac{\hat{\lambda} - \lambda_0}{\lambda_0}\right)_\text{Earth} \equiv \frac{b_\text{DM}}{c} \tag{7}$$

be the relative half-width of the absorption line at the wavelength $\hat{\lambda}$ at which the absorbed flux is reduced by a factor $1/e$ from the absorbed flux at λ_0 (see (13) below). Note that b_DM is defined with units of velocity. We have $b_\text{DM}/c \equiv (\hat{v} - v_0)/c \approx \sqrt{2} RH/c$, where $H = (\text{d}a/\text{d}t)/a = H_0 \sqrt{\Omega_m / a^3}$ is the Hubble expansion parameter. (We take R to be a standard deviation, hence the factor $\sqrt{2}$.) Let us consider a cloud with the minimum mass M_hm. We will relate R with the comoving warm dark matter root-mean-square free-streaming length l_fs (in three dimensions, or $l_\text{fs}/\sqrt{3}$ along the line of sight): $R \approx l_\text{fs} a/\sqrt{3}$. In summary, we obtain

$$b_\text{DM}^2 \approx l_\text{fs}^2 H_0^2 \Omega_m \frac{2}{3a}. \tag{8}$$

In [9], a broadening is added due to baryon Jeans pressure:

$$b_\rho^2 = f_J^2 \frac{10 k_\text{B} T}{9 \mu m_\text{H} \Delta} = (11.1\ \text{km/s})^2 \left(\frac{f_J}{0.88}\right)^2 \left(\frac{T_0}{10^4\ \text{K}}\right) \Delta^{\gamma-2}. \tag{9}$$

$f_\text{J}/0.88$ is estimated to be ≈ 1 from simulations in [9]. The expression (9) can be obtained replacing l_fs in (8) by $\approx \lambda_\text{J}/a$, with λ_J defined in Appendix E. (The extra factor Δ in the denominator depends on how fast hydrogen approaches equilibrium with the photon temperature before $z \approx 150$, see Appendix E). In my view, this term (9) is appropriate if $M_\text{J} > M$. Our case of interest is warm dark matter with $M_\text{J} \ll M_\text{hm}$, *i.e.* $k_\text{fs} \ll 150$ Mpc^{-1}, so, in this case, we omit the term (9).

The intergalactic baryons have a temperature that varies greatly between voids and filaments, so the correction from b^2 to b_DM^2 is highly uncertain, and is specific to each neutral hydrogen "cloud". We will consider two corrections as bench-marks:

$$b_{\mathrm{DM}}^2 \approx b^2 - (12.8\ \mathrm{km/s})^2 - \left(\sqrt{2}\cdot 2.55\ \mathrm{km/s/a}\right)^2, \quad \text{or} \tag{10}$$

$$b_{\mathrm{DM}}^2 \approx b^2 - (12.8\ \mathrm{km/s})^2 - \left(\sqrt{2}\cdot 2.55\ \mathrm{km/s/a}\right)^2 - (11.1\ \mathrm{km/s})^2. \tag{11}$$

(10) is our default, and (11), used in [9] and [16], will help us estimate systematic uncertainties.

5. Measurement of k_{fs} with the Lyman-α Power Spectrum

Let us consider the Lyman-α power spectrum presented in **Figure 3** (obtained in [17] from the Keck Observatory Database of Ionized Absorption toward Quasars (KODIAQ)). The redshift of the power spectrum in **Figure 3** is $z = 3.6$. This power spectrum $P_{\mathrm{1D}}(k_z)$ is compared to calculations (with (40) and (41) in Appendix F) for several density power spectra $P_{\mathrm{3D}}(k)$. A good fit (except for the last data point) is obtained with $k_{\mathrm{fs}} = 4.9\ \mathrm{Mpc}^{-1}$ (that still needs to be corrected).

This is our second lesson. The first lesson is this: dark matter is warm. This conclusion is obtained from four independent estimates that are in agreement (see **Table 3** of [2] and references therein). The second lesson is this: the observed Lyman-α forest power spectrum cut-off is mainly due to warm dark matter free-streaming. This conclusion is obtained from the agreement of $k_{\mathrm{fs}} = 4.9\ \mathrm{Mpc}^{-1}$ with the four estimates in [2]. In other words, the contribution to the Lyman-α forest power spectrum cut-off by the neutral hydrogen temperature and the baryon Jeans pressure are relatively small. This conclusion will allow us to make a new measurement of k_{fs} in spite of the uncertainties in (10) or (11).

Both the 3D density power spectrum $P_{\mathrm{3D}}(k)$ and the 1D Lyman-α power spectrum $P_{\mathrm{1D}}(k_z)$ have a cut-off. The cut-off wavevector that drops $P_{\mathrm{1D}}(k_z)$ by a factor $1/e$ is $k_{z\mathrm{fs}} = \sqrt{2}/(ab) \approx 0.0676\ \mathrm{s/km}$ (see **Figure 3**), so $ab = 20.9\ \mathrm{km/s}$. $a = 1/(1+z) = 1/(1+3.6)$. The corresponding $ab_{\mathrm{DM}} = 20.4\ \mathrm{km/s}$ assuming (10), or $ab_{\mathrm{DM}} = 20.3\ \mathrm{km/s}$ assuming (11). The corrected $k_{\mathrm{fs}} = 4.9\cdot 20.9/20.4 = 5.0\ \mathrm{Mpc}^{-1}$, or 5.1 Mpc^{-1}, respectively. So the correction is negligible.

In **Figure 4** we consider redshift $z = 4.2$ [17]. A fair fit (except for the last data point) is obtained with $k_{\mathrm{fs}} = 5.3\ \mathrm{Mpc}^{-1}$. $P_{\mathrm{1D}}(k_z)$ drops by a factor $1/e$ at $k_{z\mathrm{fs}} = \sqrt{2}/(ab) \approx 0.0832\ \mathrm{s/km}$ (see **Figure 4**), so $ab = 17.0\ \mathrm{km/s}$. The corresponding $ab_{\mathrm{DM}} = 16.5\ \mathrm{km/s}$ assuming (10), or 16.4 km/s assuming (11). The corrected $k_{\mathrm{fs}} = 5.3\cdot 17.0/16.5 = 5.5\ \mathrm{Mpc}^{-1}$, or 5.5 Mpc^{-1}, respectively.

Let us repeat this analysis with the Lyman-α power spectrum obtained in [6] at $z = 4.6$, and analyzed in [5] where a limit is obtained. We are unable to obtain a good fit using (40) and (41), see **Figure 5**.

Our final measurement is

$$k_{\mathrm{fs}} = 5.0 \pm 0.1(\mathrm{stat}) \pm 1.0(\mathrm{syst}) \pm 2.0(\mathrm{other})\,\mathrm{Mpc}^{-1}. \tag{12}$$

The statistical uncertainty is obtained from the uncertainties in [17]. The systematic uncertainty is obtained from the differences of the results for $z = 3.6$ and $z = 4.2$, with the corrections (10) and (11). The major "other" uncertainty is estimated from the discrepancy between **Figure 3** and **Figure 5**, the uncertain relation between the total density and the neutral hydrogen density, the contribution of non-expanding galaxy halos, the contribution of narrow Lyman-α absorptions that belong to larger structures (see **Figure 2**), etc. The corresponding "standard thermal relic mass" m_{th} (defined by Equations (6) and (7) of [3]) is $0.5 \lesssim m_{th} \lesssim 1.3$ keV.

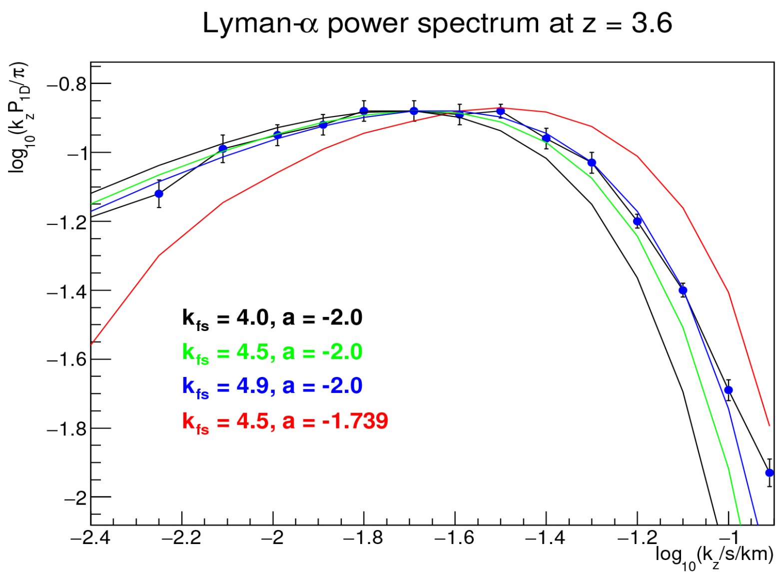

Figure 3. Measured Lyman-α dimensionless power spectrum $k_z P_{1D}(k_z)/\pi$ at $z = 3.6$ [17], compared with calculations with (40) and (41) for several $P_{3D}(k)$. A good fit is obtained with $a = -2.0$ and the cut-off wavevector $k_{fs} = 4.9$ Mpc^{-1} (blue line). Note the sensitivity to a and k_{fs}.

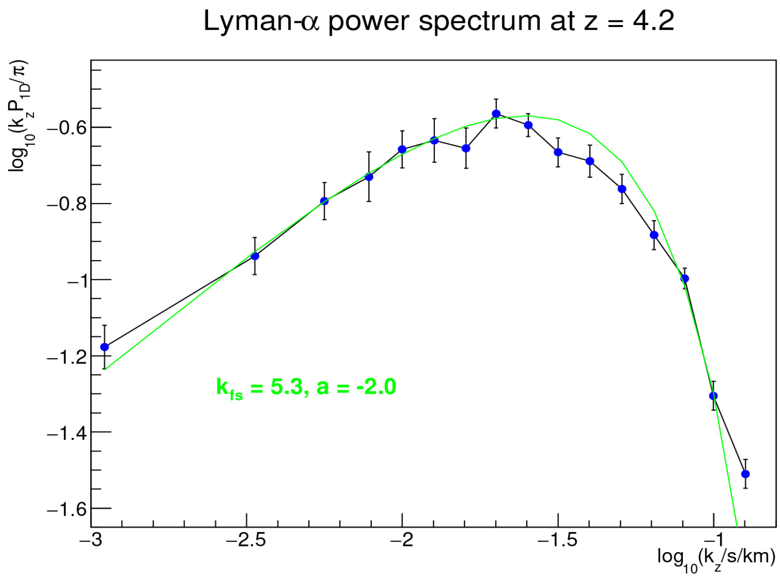

Figure 4. Measured Lyman-α dimensionless power spectrum $k_z P_{1D}(k_z)/\pi$ at $z = 4.2$ [17], compared with calculations with (40) and (41) for several $P_{3D}(k)$. A fair fit is obtained with $a = -2.0$ and the cut-off wavevector $k_{fs} = 5.3$ Mpc^{-1} (green line).

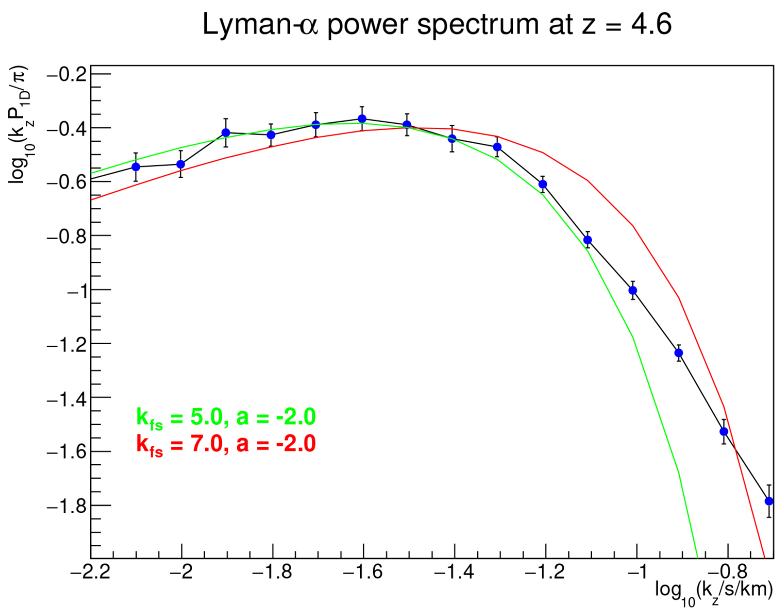

Figure 5. Measured Lyman-α dimensionless power spectrum $k_z P_{1D}(k_z)/\pi$ at $z = 4.6$ [6], compared with calculations with (40) and (41) for several $P_{3D}(k)$. Note the sensitivity to k_{fs}. We are unable to obtain a good fit.

6. Lyman-α Trees

We try a different approach: instead of the power spectrum of the "Lyman-α forest", we study individual absorption lines, *i.e.* individual "trees". As an example, consider two spectra of quasar J140501+444800, taken on May 16 and May 20, 2005, by the Keck Observatory. Most of the spectra looks like the top Figure 1. We inspect by eye the spectra from 5000 Å to 6095 Å in steps of 10 Å. We write down the wavelength, half-width, and amplitude of each absorption line that appears to be above "noise". Two example absorption lines are presented in the middle and bottom panels of Figure 1. These lines can be approximated by (we use the notation of [9])

$$F = F_0 - \Delta F \cdot \exp\left(-\frac{(\lambda-\lambda_0)^2}{\lambda_0^2}\frac{c^2}{b'^2}\right) \equiv F_0 - \Delta F \cdot \exp\left(-\frac{(v-v_0)^2}{b'^2}\right), \tag{13}$$

(we have replaced b by b' to emphasize that b' has an individual value for each Lyman-α absorption line). Note that the standard deviation of v is $\sigma = b'/\sqrt{2}$. All absorption lines that coincide between the two spectra are listed in Table 1. We note that only 10 absorption lines are found above "noise". These absorption lines are not emphasized when the power spectrum of the "Lyman-α forest" is calculated, considering that most of the spectra looks like the top Figure 1. We conclude that an alternative measurement of the dark matter warmness may focus on individual "Lyman-α trees".

Each of the absorption lines listed in Table 1 obtains "k_{fs}" if the line-of sight traverses, with no offset, an overdensity of the minimum mass M_{hm} that is still linear and expanding, see Appendix E. The challenge is to identify which absorption

Table 1. Parameters of several absorption lines of spectra of quasar J140501+444800. $b' = c\Delta\lambda/\lambda$, with half-width $\Delta\lambda$ measured at peak flux absorption times $1/e$. b_{DM} from (10), l_{fs} from (8), $v_{hrms}(1)$ from (36), and k_{fs} from (27). The calculations assume that the line-of-sight goes through the center of a linear and expanding overdensity of mass M_{hm} defined in Appendix E. The challenge is to identify an absorption line with these characteristics. Calculations correspond to (10), except the last column corresponds to (11)*.

λ [Å]	amplitude	half-width [Å]	b' [km/s]	b_{DM} [km/s]	l_{fs} [Mpc]	$v_{hrms}(1)$ [m/s]	"k_{fs}" [Mpc^{-1}]	"k_{fs}"* [Mpc^{-1}]
5067.2	12%	0.32	18.9	13.5	0.21	80	6.1	10.8
5142.3	85%	0.50	29.1	25.9	0.41	153	3.2	3.5
5341.3	85%	0.15	8.4	imaginary			infty	infty
5341.7	85%	0.25	14.0	4.5	0.07	26	19.0	infty
5343.7	99%	0.89	49.9	48.1	0.74	279	1.8	1.8
5357.3	100%	0.86	48.1	46.3	0.71	267	1.8	1.9
5451.7	60%	0.45	24.7	20.9	0.32	120	4.1	4.8
5741.3	25%	0.66	34.5	31.8	0.47	178	2.8	3.0
5930.0	22%	0.75	37.9	35.5	0.52	195	2.5	2.6
5991.6	55%	0.36	18.0	12.1	0.18	66	7.4	18.2

lines meet these requirements. The line-of-sight to the quasar generally traverses the cloud with an offset, so the observed absorption line is narrower than with no offset. Furthermore, the line-of-sight may traverse a galaxy halo that is not expanding, which again obtains a narrow absorption line. So obtaining the warmness of dark matter with the individual trees is highly non-trivial, and requires extensive simulations, but needs to be attempted. The suggestion is to study histograms of b' in bins of amplitude ΔF. Let us mention, however, that all "k_{fs}" obtained in Table 1 are consistent with the warm dark matter measured in [2], except the absorption at 5341.3 Å that happens to be part of a larger structure shown in Figure 2.

7. Conclusion

We have presented studies of the Lyman-α forest assuming dark matter is warm. The fits to the Lyman-α power spectra obtained in [17] obtain $k_{fs} \approx 5.0 \pm 2.2$ Mpc^{-1}, corresponding to a "standard thermal relic mass" $0.5\text{ keV} \lesssim m_{th} \lesssim 1.3\text{ keV}$ (defined by Equations (6) and (7) of [3]), in agreement with four independent estimates presented in [2]. In conclusion, the warm dark matter free-streaming is clearly observed as a cut-off of the Lyman-α forest power spectrum.

Acknowledgements

This research has made use of the Keck Observatory Archive (KOA), which is operated by the W. M. Keck Observatory and the NASA Exoplanet Science Institute (NExScI), under contract with the National Aeronautics and Space Administration.

Conflicts of Interest

The author declares no conflicts of interest regarding the publication of this paper.

References

[1] Navas, S., *et al.* (2024) The Review of Particle Physics. *Physical Review D*, **110**, Article ID: 030001.

[2] Hoeneisen, B. (2026) Update to Four Estimates of the Dark Matter Warmness. *International Journal of Astronomy and Astrophysics*, **16**, 79-93. https://doi.org/10.4236/ijaa.2026.162006

[3] Viel, M., Lesgourgues, J., Haehnelt, M.G., Matarrese, S. and Riotto, A. (2005) Constraining Warm Dark Matter Candidates Including Sterile Neutrinos and Light Gravitinos with WMAP and the Lyman-α Forest. *Physical Review D*, **71**, Article ID: 063534. https://doi.org/10.1103/physrevd.71.063534

[4] Liu, B., Shan, H. and Zhang, J. (2024) New Galaxy UV Luminosity Constraints on Warm Dark Matter from JWST. *The Astrophysical Journal*, **968**, Article 79. https://doi.org/10.3847/1538-4357/ad4ed8

[5] Iršič, V., Viel, M., Haehnelt, M.G., Bolton, J.S., Molaro, M., Puchwein, E., *et al.* (2024) Unveiling Dark Matter Free Streaming at the Smallest Scales with the High Redshift Lyman-α Forest. *Physical Review D*, **109**, Article ID: 043511. https://doi.org/10.1103/physrevd.109.043511

[6] Boera, E., Becker, G.D., Bolton, J.S. and Nasir, F. (2019) Revealing Reionization with the Thermal History of the Intergalactic Medium: New Constraints from the Lyα Flux Power Spectrum. *The Astrophysical Journal*, **872**, Article 101. https://doi.org/10.3847/1538-4357/aafee4

[7] Dekker, H., D'Odorico, S., Kaufer, A., Delabre, B. and Kotzlowski, H. (2000) Design, Construction, and Performance of UVES, the Echelle Spectrograph for the UT2 Kueyen Telescope at the ESO Paranal Observatory. *SPIE Proceedings*, **4008**, 534-545. https://doi.org/10.1117/12.395512

[8] Vogt, S.S., Allen, S.L., Bigelow, B.C., Bresee, L., Brown, W.E., Cantrall, T., *et al.* (1994) HIRES: The High-Resolution Echelle Spectrometer on the Keck 10-m Telescope. *SPIE Proceedings*, **2198**, 362. https://doi.org/10.1117/12.176725

[9] Garzilli, A., Theuns, T. and Schaye, J. (2015) The Broadening of Lyman-α Forest Absorption Lines. *Monthly Notices of the Royal Astronomical Society*, **450**, 1465-1476. https://doi.org/10.1093/mnras/stv394

[10] MacInnis, A. and Sehgal, N. (2025) CMB-HD as a Probe of Dark Matter on Sub-Galactic Scales. *Journal of Cosmology and Astroparticle Physics*, **2025**, Article 48. https://doi.org/10.1088/1475-7516/2025/02/048

[11] Broxterman, J.C., Simon, P., Porth, L., Kuijken, K., Wright, A.H., Asgari, M., *et al.* (2025) Matter Power Spectrum Reconstruction with Kids-Legacy: Improved Internal ΛCDM Consistency and Preference for Strong Baryonic Feedback. *Astronomy & Astrophysics*, **703**, L3. https://doi.org/10.1051/0004-6361/202557182

[12] Perez Sarmiento, K., Laguë, A., Madhavacheril, M.S., Jain, B. and Sherwin, B. (2025) Reconstructing the Shape of the Nonlinear Matter Power Spectrum Using CMB Lensing and Cosmic Shear. *Physical Review D*, **112**, Article ID: 063510. https://doi.org/10.1103/bzrj-76sn

[13] O'Meara, J.M., Lehner, N., Howk, J.C., Prochaska, J.X., Fox, A.J., Peeples, M.S., *et al.* (2017) The Second Data Release of the KODIAQ Survey. *The Astronomical Journal*,

154, Article 114. https://doi.org/10.3847/1538-3881/aa82b8

[14] O'Meara, J.M., Lehner, N., Howk, J.C., Prochaska, J.X., Fox, A.J., Swain, M.A., *et al.* (2015) The First Data Release of the Kodiaq Survey. *The Astronomical Journal*, **150**, Article 111. https://doi.org/10.1088/0004-6256/150/4/111

[15] Lehner, N., O'Meara, J.M., Fox, A.J., Howk, J.C., Prochaska, J.X., Burns, V., *et al.* (2014) Galactic and Circumgalactic O Vi and Its Impact on the Cosmological Metal and Baryon Budgets AT $2 < z \lesssim 3.5$. *The Astrophysical Journal*, **788**, Article 119. https://doi.org/10.1088/0004-637x/788/2/119

[16] Garzilli, A., Magalich, A., Theuns, T., Frenk, C.S., Weniger, C., Ruchayskiy, O., *et al.* (2019) The Lyman-α Forest as a Diagnostic of the Nature of the Dark Matter. *Monthly Notices of the Royal Astronomical Society*, **489**, 3456-3471. https://doi.org/10.1093/mnras/stz2188

[17] Göksel Karaçayl, N., Padmanabhan, N., Font-Ribera, A., *et al.* (2022) Optimal 1D Lyα Forest Power Spectrum Estimation—II. KODIAQ, SQUAD & XQ-100, arxiv:2108.10870.

[18] Hoeneisen, B. (2025) The Warm Dark Matter Plus Baryon Linear Power Spectrum. *International Journal of Astronomy and Astrophysics*, **15**, 264-281. https://doi.org/10.4236/ijaa.2025.153017

[19] Boyanovsky, D., de Vega, H.J. and Sanchez, N.G. (2008) Dark Matter Transfer Function: Free Streaming, Particle Statistics, and Memory of Gravitational Clustering. *Physical Review D*, **78**, Article ID: 063546. https://doi.org/10.1103/physrevd.78.063546

[20] Macciò, A.V., Paduroiu, S., Anderhalden, D., Schneider, A. and Moore, B. (2012) Cores in Warm Dark Matter Haloes: A Catch 22 Problem. *Monthly Notices of the Royal Astronomical Society*, **424**, 1105-1112. https://doi.org/10.1111/j.1365-2966.2012.21284.x

[21] Weinberg, S. (2008) Cosmology. Oxford University Press.

Appendix A. Definition of Dark Matter Warmness

The dark matter warmness can be defined by any of these variables: the comoving root-mean-square dark matter thermal velocity $v_{hrms}(1)$, the comoving power spectrum cut-off wavevector k_{fs}, the "standard thermal relic mass" m_{th} defined by Equations (6) and (7) of [3], or the expansion parameter at which dark matter becomes non-relativistic, defined as $a_{\text{NR}} \equiv v_{hrms}(1)/c$. The comoving power spectrum of relative density perturbations of the cold dark matter ΛCDM cosmology becomes attenuated by a cut-off factor $\tau^2(k)$ if dark matter is warm: $P(k)_{\Lambda\text{WDM}} = P(k)_{\Lambda\text{CDM}}\tau^2(k)$. k is the comoving wavevector. To be specific we assume a Maxwell-Boltzmann distribution of warm dark matter velocities. In this case $\tau^2(k)$ has the approximate form $\tau^2(k) = \exp\left(-k^2/k_{\text{fs}}^2\right)$ [18], so $\tau^2(k_{\text{fs}}) \equiv \exp(-1)$. This is our definition of k_{fs}. (Other definitions in the literature are $\tau^2(k_{\text{fs}}) = 1/2$ or 1/4.) A handy table relating these parameters is Table 1 of [2].

Appendix B. The Lyman-α 1D Power Spectrum Notation

The observed flux $F\left((\lambda-\lambda_0)c/\lambda_0\right) \equiv F(v)$ and its mean $\langle F\rangle$ define the normalized flux

$$\delta_F(v) \equiv \frac{F(v)-\langle F\rangle}{\langle F\rangle}. \tag{14}$$

Consider a large velocity interval (0, $\mathcal{V}$), and apply periodic boundary conditions. Then we may write

$$\delta_F(v) = \sum_j \tilde{\delta}_F(k_{zj})\mathrm{e}^{ik_{zj}v}, \quad \tilde{\delta}_F(k_{zj}) = \frac{1}{\mathcal{V}}\int_0^{\mathcal{V}} \mathrm{d}v\mathrm{e}^{-ik_{zj}v}\delta_F(v), \tag{15}$$

with $k_{zj} = j2\pi/\mathcal{V}$. The power spectrum and dimensionless variance are defined as

$$P_{\text{1D}}(k_{zj}) \equiv \mathcal{V}\sum_j \left|\tilde{\delta}_F(k_{zj})\right|^2, \quad \Delta_{\text{1D}}^2(k_{zj}) \equiv \frac{k_{zj}}{\pi}P_F(k_{zj}). \tag{16}$$

Appendix C. Relation between Free-Streaming and the Power Spectrum Cut-Off

We use the notation of [1]. The relative density perturbation is

$$\delta(\boldsymbol{x}) \equiv \frac{\rho(\boldsymbol{x})-\langle\rho\rangle}{\langle\rho\rangle}, \tag{17}$$

where $\langle\rho\rangle$ is the root-mean-square of $\rho(\boldsymbol{x})$. The Fourier transform pair, with periodic boundary conditions on a cube of volume V, is

$$\delta(\boldsymbol{x}) = \sum \delta_{\boldsymbol{k}}\mathrm{e}^{-i\boldsymbol{k}\cdot\boldsymbol{x}}, \quad \delta_{\boldsymbol{k}} = \frac{1}{V}\int \delta(\boldsymbol{x})\mathrm{e}^{i\boldsymbol{k}\cdot\boldsymbol{x}}\mathrm{d}^3\boldsymbol{x}. \tag{18}$$

The power spectrum is defined by

$$\left\langle \delta^2 \right\rangle = \sum \left| \delta_k \right|^2 \equiv \sum P(k). \tag{19}$$

In the end we take the limit $V \to \infty$.

If dark matter is warm instead of cold, dark matter particles free-stream into, and out of, density minimums and maximums, attenuating small scale perturbations. Then the cold dark matter relative density perturbation becomes smoothed by a convolution with a cut-off function $\Phi(\boldsymbol{x})$:

$$\delta_{\mathrm{WDM}}(\boldsymbol{x}) = \int \delta_{\mathrm{CDM}}(\boldsymbol{y}) \phi(\boldsymbol{x} - \boldsymbol{y}) \mathrm{d}^3 \boldsymbol{y}. \tag{20}$$

The Fourier transform of a convolution is equal to the product of Fourier transforms. Therefore, the warm and cold dark matter power spectra are related by

$$P_{\mathrm{WDM}}(k) = P_{\mathrm{CDM}}(k) \tau^2(k), \tag{21}$$

where $\tau^2(k)$ is a cut-off factor, and $\tau(\boldsymbol{k})$ is the Fourier transform of $\phi(\boldsymbol{x})$.

We first study the case of a Gaussian cut-off function with zero mean:

$$\phi(\boldsymbol{x}) = \frac{2^{3/2}}{\pi^{3/2} \sigma^3} \exp\left[-\frac{r^2}{2\sigma^2} \right] = \int \frac{\mathrm{d}^3 \boldsymbol{k}}{(2\pi)^3} \tau(\boldsymbol{k}) \mathrm{e}^{-i\boldsymbol{k} \cdot \boldsymbol{x}} \tag{22}$$

where $r = |\boldsymbol{x}|$, $\sigma \equiv l_{\mathrm{fs}}$ is the root-mean-square free-streaming distance, and

$$\tau(\boldsymbol{k}) = \tau(k) = \int \phi(\boldsymbol{x}) \mathrm{e}^{i\boldsymbol{k} \cdot \boldsymbol{x}} \mathrm{d}^3 \boldsymbol{x} = \exp\left[-\frac{k^2 \sigma^2}{2} \right] \equiv \exp\left[-\frac{k^2}{2k_{\mathrm{fs}}^2} \right]. \tag{23}$$

For this Gaussian cut-off

$$P_{\mathrm{WDM}}(k) = P_{\mathrm{CDM}}(k) \exp\left[-k^2 / k_{\mathrm{fs}}^2 \right], \text{ with } k_{\mathrm{fs}} = 1/\sigma = 1/l_{\mathrm{fs}}. \tag{24}$$

Let us now assume a Maxwell-Boltzmann distribution of velocities with zero chemical potential. Then

$$\phi(\boldsymbol{x}) \equiv \phi(r) \propto v^2 \exp\left[-\frac{3v^2}{2\sigma^2} \right], \tag{25}$$

with $Bv \equiv r$, and where $\sigma \equiv \sqrt{3kT/m_h} \equiv v_{h\mathrm{rms}}(1)$ is the comoving root-mean-square dark matter thermal velocity. With the definitions $R \equiv \sqrt{3} r / \left(\sqrt{2} B \sigma \right)$ and $C \equiv k \sqrt{2/3} B \sigma$, we obtain

$$\tau(\boldsymbol{k}) \equiv \tau(k) \propto \int_0^\infty R^4 \mathrm{d}R \int_{-1}^{+1} \mathrm{d}\cos(\theta) \exp\left[-R^2 \right] \mathrm{e}^{iCR\cos\theta}. \tag{26}$$

We evaluate this integral numerically, and obtain C such that $\left| \tau(k_{\mathrm{fs}}) \right|^2 / \left| \tau(0) \right|^2 = e^{-1}$. We obtain $C = 1.072$, so

$$k_{\mathrm{fs}} = \frac{1.31}{l_{\mathrm{fs}}}. \tag{27}$$

With $l_{\mathrm{fs}} = B\sigma \equiv B v_{h\mathrm{rms}}(1) \approx 0.32\ \mathrm{Mpc}\, v_{h\mathrm{rms}}(1) / 120\ \mathrm{m/s}$, (see Appendix D), we obtain

$$k_{\mathrm{fs}} = 0.62 \sqrt{\frac{4\pi G \Omega_m \rho_{\mathrm{crit}} a_{\mathrm{eq}}}{v_{h\mathrm{rms}}^2(1)}} = 4.1\ \mathrm{Mpc}^{-1} \frac{120\ \mathrm{m/s}}{v_{h\mathrm{rms}}(1)}. \tag{28}$$

When baryons are included we obtain [18]

$$k_{\text{fs}} = 0.88\sqrt{\frac{4\pi G\Omega_m \rho_{\text{crit}} a_{\text{eq}}}{v_{h\text{rms}}^2(1)}} = 5.8\ \text{Mpc}^{-1}\frac{120\ \text{m/s}}{v_{h\text{rms}}(1)}. \tag{29}$$

Figure 5 of [19] obtains

$$k_{\text{fs}} = 1.03\sqrt{\frac{4\pi G\Omega_m \rho_{\text{crit}} a_{\text{eq}}}{v_{h\text{rms}}^2(1)}} = 6.8\ \text{Mpc}^{-1}\frac{120\ \text{m/s}}{v_{h\text{rms}}(1)}. \tag{30}$$

Appendix D. Dark Matter Free-Streaming

The evolution of the universe is described by

$$H^2 \equiv \left(\frac{\mathrm{d}a/\mathrm{d}t}{a}\right)^2 = H_0^2\left(\frac{\Omega_m}{a^3} + \frac{\Omega_r}{a^4} + \Omega_\Lambda\right). \tag{31}$$

For the standard notation and parameter values, see [1]. The warm dark matter comoving free-streaming root-mean-square distance is

$$l_{\text{fs}} = \int_0^{t_e} \mathrm{d}t' \frac{c}{a(t')} \frac{p}{\sqrt{p^2 + a(t')^2 m_h^2 c^2}}. \tag{32}$$

$a(t)$ is the expansion parameter normalized to $a(t_0) = 1$ at the present time t_0. $\boldsymbol{p}$ is the comoving momentum, and m_h is the dark matter particle mass. The proper root-mean-square non-relativistic dark matter particle velocity at expansion parameter a is $v_{h\text{rms}}(a)$. The comoving root-mean-square non-relativistic dark matter particle velocity $v_{h\text{rms}}(1) = v_{h\text{rms}}(a)a = p_{h\text{rms}}(1)/m_h$ is an adiabatic invariant. In the present article we integrate (32) numerically.

To understand the relation between l_{fs} and $v_{h\text{rms}}(1)$ it is convenient to have an approximate analytic equation. Carrying out the integral in 3 intervals from 0 to a_{NR}, a_{NR} to a_{eq}, and a_{eq} to 1, obtains approximately

$$l_{\text{fs}} \approx \frac{v_{h\text{rms}}(1)}{H_0\sqrt{\Omega_r}} + \frac{v_{h\text{rms}}(1)}{H_0\sqrt{\Omega_r}}\ln\left(\frac{ca_{\text{eq}}}{v_{h\text{rms}}(1)}\right) + \frac{2v_{h\text{rms}}(1)}{H_0\sqrt{\Omega_m a_{\text{eq}}}}. \tag{33}$$

As an example, the three terms in (33), for $v_{h\text{rms}}(1) = 120$ m/s, are

$$l_{\text{fs}} \approx (0.19 + 1.22 + 0.37)\text{Mpc}. \tag{34}$$

For comparison, the numerical integral obtains

$$l_{\text{fs}} = (0.16 + 1.12 + 0.32)\text{Mpc}. \tag{35}$$

We now argue that we should keep only the last term in (35), *i.e.*

$$l_{\text{fs}} \approx 0.32\ \text{Mpc}\frac{v_{h\text{rms}}(1)}{120\ \text{m/s}} = \frac{0.32}{0.37}\frac{2v_{h\text{rms}}(1)}{H_0\sqrt{\Omega_m a_{\text{eq}}}} = 2.12\sqrt{\frac{v_{h\text{rms}}^2(1)}{4\pi G\Omega_m \rho_{\text{crit}} a_{\text{eq}}}}. \tag{36}$$

Consider the interval from a_{NR} to a_{eq}. From Equation (29) of [18], the difference between cold and warm dark matter only occurs at $k > k_{\text{Jh}}$, and in this regime the free-streaming of warm dark matter is oscillatory. We also neglect the contribution from the interval 0 to a_{NR}: for $t < t_{\text{NR}}$ all particles are ultra-relativistic, so the dark matter makes no difference. What is of interest are the "initial" perturbations at $t = t_{eq}$. Note that the result (36) is only used to obtain $v_{hrms}(1)$, not k_{fs} nor m_{th}: the uncertainty due to l_{fs} is added only to $v_{hrms}(1)$.

Appendix E. The Masses M_{hm} and M_J

From simulations in [20] we find that, given the comoving warm dark matter free-streaming cut-off wavevector k_{fs}, the minimum total (warm dark matter plus baryon) mass that collapses due to gravity is

$$M_{hm} \approx \frac{4}{3}\pi\left(\frac{2.3}{k_{fs}}\right)^3 \Omega_m \rho_{crit}. \tag{37}$$

Another mass of interest is a sort of Jeans mass [21]

$$M_J = \left(\frac{\pi}{G}\right)^{3/2} \frac{v_s^3}{\bar{\rho}_M^{1/2}} \equiv \lambda_J^3 \Omega_m \rho_{crit} (1+z)^3, \tag{38}$$

where $\bar{\rho}_M$ is the total (dark matter plus baryon) mean density at expansion parameter a, and

$$v_s = \frac{\partial P_B}{\partial \rho_B} = \left(\frac{5 k_B T}{3 \mu m_N}\right)^{1/2} \tag{39}$$

is the sound velocity of the plasma at expansion parameter a, with $\mu = 1.22$ for 24 % helium by weight. It turns out that, due to residual ionization, baryons stay in thermal equilibrium with photons until about $z \approx 150$ [21], so the baryon temperature $T = T_\gamma$, $T_\gamma^3 / \bar{\rho}_M$ has its present value, and $M_J = 6 \times 10^5\ M_\odot$, until $z \approx 150$. (After re-ionization, we take $\mu = 0.59$ [9].)

We note that $M_{hm} = M_J$ if $k_{fs} = 150\ \text{Mpc}^{-1}$. So, the minimum matter that will collapse gravitationally is M_{hm}, and this matter collapses with a full complement of baryons only if $M_{hm} \gtrsim M_J$ or $k_{fs} \lesssim 150\ \text{Mpc}^{-1}$.

If dark matter is warm with $k_{fs} \ll 150\ \text{Mpc}^{-1}$ (our scenario of interest) we will treat matter (dark matter plus baryons) as a single fluid collapsing gravitationally. If dark matter is colder with $k_{fs} \gtrsim 150\ \text{Mpc}^{-1}$ the baryon plasma needs to be considered separately.

Appendix F. From $P_{3D}(k)$ to $P_{1D}(k_z)$

The predicted 1D Lyman-α power spectrum can be obtained from the 3D density power spectrum as follows:

$$P_{1D}(k_z) dk_z = \int P_{3D}(k) dk_z 2\pi k \sin\theta \frac{k d\theta}{\cos\theta},$$

$$P_{1D}(k_z) = \int_{k_z}^{\infty} -P_{3D}(k) 2\pi k dk. \tag{40}$$

The 3D density power spectrum, in the range of k of interest, has the form

$$P_{3D}(k) \propto \left(\frac{k}{6\ \text{Mpc}^{-1}}\right)^a \exp\left(-\frac{k^2}{k_{fs}^2}\right). \tag{41}$$

$a = -1.739$ for the measured power spectrum that includes non-linear regeneation. A good fit to the Lyman-α measurements in [17] at redshift $z = 3.6$ or 4.2 is obtained with $a = -2.0$. This is the predicted slope for the linear power spectrum, which is perhaps more appropriate for the inter-galactic medium. See **Figure 3**.